Results on Rapid 3D Magnetic Particle Imaging with a Large Field of View

J. Rahmer[1], B. Gleich[1], C. Bontus[1], I. Schmale[1], J. Schmidt[1], J. Kanzenbach[1], O. Woywode[2], J. Weizenecker[3], and J. Borgert[1]
[1]Philips Research Laboratories, Hamburg, Germany, [2]Philips Medical Systems DMC GmbH, Hamburg, Germany, [3]University of Applied Sciences, Karlsruhe, Germany

Introduction

Magnetic particle imaging (MPI) is a new tomographic imaging approach that quantitatively maps concentrations of iron oxide nanoparticle distributions [1]. It combines high sensitivity [2,3] with the ability of fast volumetric imaging. *In vivo* 3D real-time MPI of a bolus of particles flowing through the heart and lung of mice has been demonstrated [4], but with an imaging approach that is limited to small fields of view (FoVs). A new scanner type with a bore diameter of 12 cm allowing rapid imaging with enlarged FoVs has been developed [5]. This contribution describes the sequences used for imaging of large FoVs and presents initial phantom results acquired on the new system.

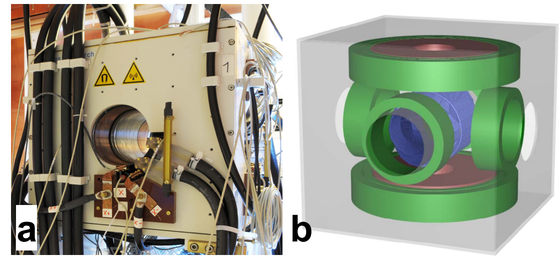

Figure 1: Fast MPI demonstrator with enlarged FoV. Photograph (a) and sketch (b) of field-generating unit, showing selection field magnets (red), focus field coils (green), and drive coils (blue).

Methods

MPI detects the non-linear response of iron-oxide nanoparticles to applied oscillating fields over a broad frequency range. Spatial encoding is achieved using a *selection field* that confines the signal to a small region, called the *field-free point* (FFP). The FFP is rapidly moved over a small volume using *drive fields*, allowing 3D spatial encoding. With this approach, a first MPI prototype was capable of 3D imaging at a rate of 46 volumes per second for a FoV of 16.8 × 20.4 × 12.0 mm [4]. Larger imaging volumes would require higher drive fields, which could lead to patient heating in a clinical scenario. To overcome this problem, additional *focus field* (FF) coils have been integrated in a new preclinical demonstrator (PCD), cf. Fig. 1 [5]. The focus fields move the rapidly encoded small volume continuously or step-wise through space to increase spatial coverage up to (10 cm)³. The selection field magnets generate constant gradients $dB_z/dz = 2.50$ T/m and $dB_x/dx = dB_y/dy = 1.25$ T/m, and the drive coils apply sinusoidal fields with amplitudes $B_{Dx} = B_{Dy} = B_{Dz} = 11$ mT at frequencies 25.3, 26.0, and 24.5 kHz for the x, y, and z channel, respectively. These fields move the FFP in a dense pattern over a box-shaped volume of 17.6 × 17.6 × 8.8 mm³ with a repetition time of TR = 21.5 ms. For the phantom scans, the FF is operated step-wise with two different sequences: (a) 3 stations with respective shifts of 12 mm in *x* direction, so that the *x* FoV extends over 41.6 mm. (b) 3 × 2 × 2 stations in the *x*, *y*, and *z* direction with shifts leading to a FFP volume coverage of 34.5 × 24.3 × 17.0 mm³. At each FF station, two 3D trajectory cycles with duration 21.5 ms were performed, but only the 2nd one was used, since during the 1st one, the FF was changed and needed time to settle to the new value. Thus, the 3-station sequence has a TR of 6 × 21.5 ms = 129 ms, whereas the 12 station sequence has TR = 517 ms. During each TR, a full 3D image is encoded. During 5-minute scans, 4D data with several hundred volumes were acquired. For signal reception, 3-channel insert coils were used. A small coil for the 3-station scan had a length of 50 mm and a diameter of 45 mm, a larger coil for the 12-station scan had a length of 80 mm and a diameter of 65 mm. Scans were performed on phantoms filled with iron particles (Resovist, Bayer Schering Pharma AG, Germany) [6] at a concentration of 25 mM(Fe)/l.

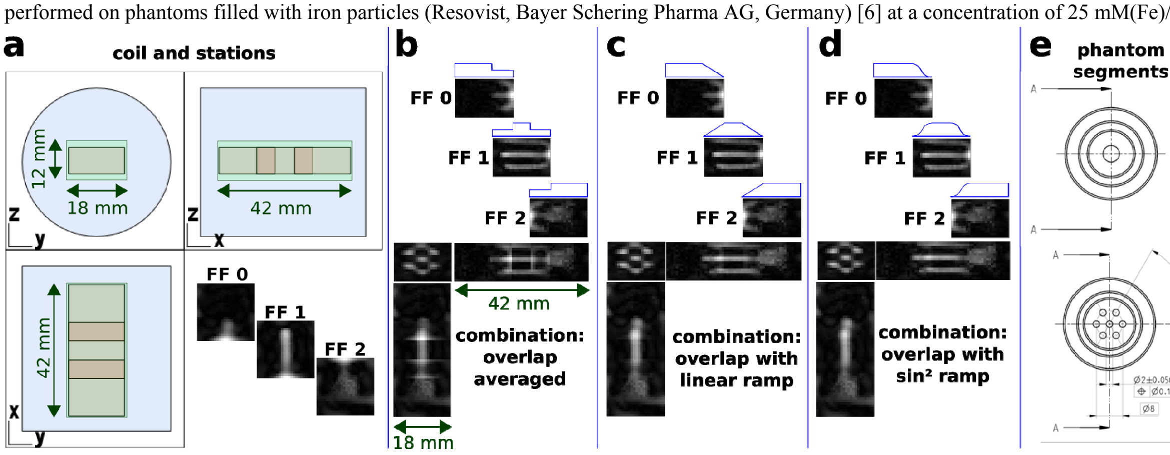

Figure 2: Coil, FF stations and combination of images from 3 stations. (a) Orthoview of area inside receive coil (blue), 3 overlapping FF stations (red), and reconstructed FoV (green). (b-d) Combination of separately reconstructed stations of a volume with different overlap weighting profiles, as shown in blue over the xz single station images. (e) The phantom consisted of two segments, with a single tube (∅ = 5 mm) and 7 tubes (∅ = 2 mm), respectively.

Results and Discussion

Figure 2 shows *xy* and *xz* slices of 3 separately reconstructed FF stations and their combination in image space. The 3 sub-volumes were acquired in one TR of the 3-station FF sequence. Since some signal from outside the station accumulates at the edge of the FoV, it is necessary to reduce the weight of the edge signal to avoid stitching artifacts (cf. Fig. 2(c,d) vs. (b)). This can be done using weighting profiles (Fig.2 (c,d)). However, some distortions remain, which may be due to the fact that the reconstructed volume is slightly larger than the volume actually covered and encoded by the FFP.

Figure 3 shows a 3D rendering of one volume reconstructed from the 12-station scan. The stations have been combined using the linear ramp approach in the overlapping parts. Different tubes of the phantom with a minimal separation of 2 mm are resolved.

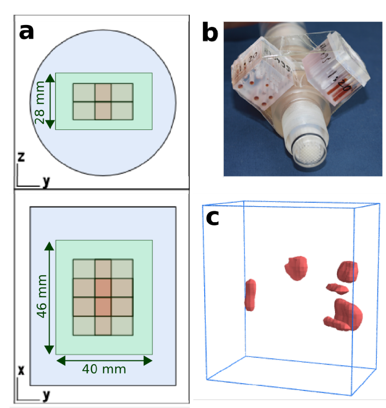

Figure 3: Coil, FF stations and combination of stations. (a) Area inside receive coil (blue), overlapping FF stations (red), and reconstructed FoV (green). (b) Phantom. (c) Rendering of 3D volume after combination of stations.

Conclusion

With a multi-station approach using focus fields, the accessible imaging volume for rapid MPI can be increased without increasing the energy deposition in the object. The acquisition time per volume is proportional to the number of stations. Care must be taken to avoid stitching artifacts, when the sub-volumes are combined into a large image. Other sequences with continuous focus field variation will be implemented in the future.

Acknowledgement

This work was funded by the German Federal Ministry of Education and Research (BMBF, grant FKZ 13N9079).

References

[1] Gleich B and Weizenecker J. Nature 435:1214-1217 (2005). [2] Weizenecker J, Borgert J, and Gleich B. Phys. Med. Biol. 53:N81-N84 (2008). [3] Goodwill PW, Scott GC, Stang PP, and Conolly SM. IEEE Trans. Med. Imag. 28:1231-7 (2009). [4] Weizenecker J, Gleich B, Rahmer J, Dahnke H, and Borgert J. Phys. Med. Biol. 54:L1-L10 (2009). [5] Gleich B *et al.* Proc. Intl. Soc. Mag. Reson. Med. 18:218 (2010). [6] Lawaczeck R *et al.* Acta Radiologica (Stockholm, Sweden: 1987) 38: 584-597 (1997).